Chinese Chemical Letters 32 (2021) 3487–3490

Contents lists available at ScienceDirect

Chinese Chemical Letters

journal homepage: www.elsevier.com/locate/cclet

Communication

Novel photo-theranostic GdB_6 nanoparticles for fluorescence imaging and NIR-photothermal therapy

Yuqi Chen[a], Mengna Jiang[a], Liwei Xiong[b], Xianxian Yao[a], Mingjian Fan[a], Danyang Chen[a], Qi Jiang[a], Zhaokui Jin[a], Qianjun He[a,*]

[a] Guangdong Provincial Key Laboratory of Biomedical Measurements and Ultrasound Imaging, National-Regional Key Technology Engineering Laboratory for Medical Ultrasound, Marshall Laboratory of Biomedical Engineering, School of Biomedical Engineering, Health Science Center, Shenzhen University, Shenzhen 518060, China

[b] Hubei Key Laboratory of Plasma Chemistry and Advanced Materials, Wuhan Institute of Technology, Wuhan 430205, China

ARTICLE INFO

Article history:
Received 12 January 2021
Revised 6 April 2021
Accepted 18 April 2021
Available online 24 April 2021

Keywords:
Gadolinium boride
Nanomedicine
Photothermal therapy
Fluorescence imaging
Theranostics

ABSTRACT

The development of multifunctional theranostic nano-agents is an important resolution for personalized treatment of cancer. In this work, we synthesized a new kind of gadolinium boride nanoparticles (GBN) by a microwave-assisted chemical etching method, and discovered their optical characteristics including fluorescence imaging and near-infrared (NIR) photothermal conversion capability. Bright greenishyellow fluorescence enabled for intracellular localization, while effective NIR-photothermal conversion supported photothermal therapy (PTT). *In vitro* and *in vivo* results indicated that GBN exhibited a superior antitumor performance and high biocompatibility. This study demonstrated a promising multifunctional theranostic nanoplatform for cancer treatment.

Theranostic involving the integration of diagnosis and treatment is becoming more and more important to enhance the outcome and bring higher benefits for patient [1–3]. Laser is being widely applied in clinic for disease treatments owing to its advantages in facile manipulation and easy focus. Photo-theranostic agents, including photothermal and photodynamic agents for therapy, and fluorescent and photoacoustic contrast agents for imaging, have been intensively developed for cancer theranostic [4–13]. The integration of multiple photo-theranostic functions into a nanoplatform is important but still challenging, especially simultaneous possession of fluorescence photothermal effects.

Recently, two-dimensional metal borides (MBenes) with a similar structure to MXenes have been developed for use in the biomedical field owing to their unique photothermal effect and hydrogen-generating properties [14–17]. In nanoscale, there possibly are potential physicochemical properties of MBenes, attracting great interests for exploitation. Unexpectedly, we here discovered that GdB_6 nanoparticles (GBN) have both photothermal conversion capability and unique fluorescence property for the first time, in great support of cancer theranostics.

GdB_6 is a superhard and ultrastable material with two elemental layers and the interlayer connection based on intense ionic bonding, which makes it hard to be exfoliated into nanomaterials [18–21]. In this work, we developed a microwave-assisted chemical etching method to synthesize GBN. Herein, we used acetic acid and hydrogen peroxide as tow etching agents to exfoliate gadolinium and boron layers under the assistance of microwave heating. Moderate amounts of acetic acid and hydrogen peroxide were used to break the interlayer metal-boron binding under assistance of microwave. From Figs. 1a and c, as-synthesized GBN was about 180 nm in diameter. XRD data (Fig. S1 in Supporting information) indicated that the obtained GBN maintained the crystal structure of GdB_6 (JCPDF card No. 38-1462). High-resolution TEM results (Fig. 1b) further demonstrated well-defined the crystal structure of GdB_6. From Fourier transform infrared spectroscopy (FT-IR) results in Fig. S2 (Supporting information), we can find that PVP successfully modified GBN by surface coordination, in favor of good particle dispersion, as suggested by DLS data (Fig. 1c). Surprisingly, GBN exhibited a fluorescence property with bright greenish yellow fluorescence emission (Fig. 1d). Such a fluorescence feature was possibly used for cellular fluorescence imaging. In addition, fluorescence characteristic has not been found in other metal borides yet.

As to a photothermal agent, extinction coefficient and photothermal conversion efficiency (η), which reflect the abilities of absorbing light and converting light energy into thermal energy,

* Corresponding author.
E-mail address: nanoflower@126.com (Q. He).

https://doi.org/10.1016/j.cclet.2021.04.036
1001-8417/

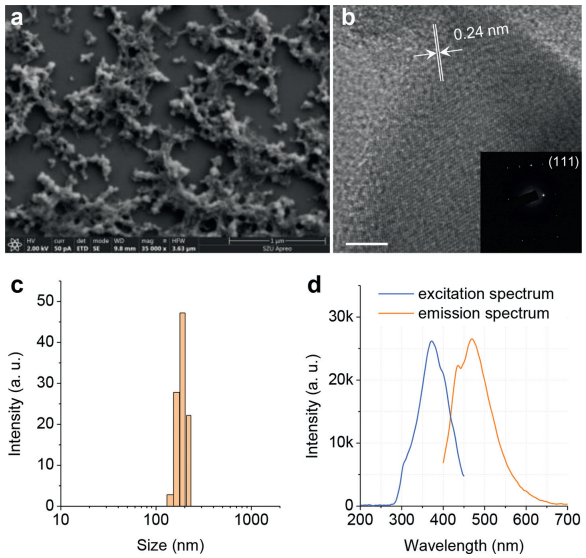

Fig. 1. Synthesis and characterization of GBN. SEM (a) and HR-TEM (b) images of GBN, DLS data of GBN (c), and fluorescence spectra of GBN (d) (For interpretation of the references to color in this figure, the reader is referred to the web version of this article.).

respectively, are two decisive parameters that determine the hyperthermia performance [5,22,23]. From Figs. 2a, GBN showed a board absorption band from UV to NIR, and its absorbance depended on its concentration. NIR-photothermal conversion efficiency (η) of GBN was measured to be 24% by the Roper method (Fig. S3 in Supporting information) [24,25]. After 4 cycles of laser switching on/off, GBN demonstrated high photothermal stability (Fig. S4 in Supporting information), ensuring the sustainable/repeatable photothermal therapy. Additionally, the photothermal performance of GBN was evaluated under irradiation of 808 nm laser at different power densities with the aqueous solution of GBN at different concentrations. From Figs. 2b and c, the photothermal effect of GBN was dependent on both the concentration of particle and the power density of light. Typically, the temperature could increase by 19.3 °C after 1 W/cm^2 NIR irradiation of 400 μg/mL GBN for 5 min. Furthermore, *in vivo* NIR-photothermal effect of GBN was investigated with a 4T1 tumor-bearing mouse model. From Figs. 2d and e, the temperature in the tumor site of mice injected with GBN rapidly increased by 35 °C after 5 min NIR irradiation, which was much more remarkable than the case of blank control treated with PBS. In addition, the intratumoral temperature change during NIR irradiation (Fig. 2d) was much higher than the *in vitro* case (Fig. 2b), possibly owing to much higher intratumoral concentration of GBN than 400 μg/mL. Such a distinct NIR-photothermal effect *in vivo* would ensure the application of GBN for NIR-photothermal therapy. Furthermore, based on NIR-photothermal effect, GBN also exhibited high NIR-photoacoustic imaging performances *in vitro* (Fig. S5 in Supporting information) and *in vivo* (Fig. S6 in Supporting information) in support of tumor diagnosis. All animal experiments were conducted under the Guide for the Care and Use of Laboratory Animals, which was approved by the Animal Experimentation Ethics Committee of Shenzhen University.

The *in vitro* cytotoxicity of GBN to cancer cells was measured using a standard CCK-8 assay and their NIR-photothermal therapy effects were evaluated *in vitro*. As a theranostic nano-agent, the cellular uptake of GBN was investigated first. From confocal images in Fig. 3a, it could be found that the GBN was easily taken up by 4T1 cells after 3 h incubation, owing to small particle size. To further investigate the localization inside the cells, lysosome was stained by Lyso-Tracker Red. It could be found that Lyso-Tracker Red staining demonstrated a high colocalization of GBN with lysosomes, suggesting that GBN was effectively endocytosed through capture by lysosomes and then escape from them to cytoplasm. This suggests that GBN can be used to trace tumor cells by fluorescence imaging and to mediate cancer therapy effectively. From Fig. 3b, higher particle concentration under NIR irradiation with the same power density could cause higher cytotoxicity to 4T1 cells. Meanwhile, 5 min NIR irradiation on GBN-treated 4T1 cells could induce the obvious apoptosis of 4T1 cells as indicated by live/dead cell staining results in Fig. 3c.

Furthermore, we performed *in vivo* photothermal therapy on 4T1 tumor-bearing mice. When the subcutaneously inoculated tumors reached around 100 mm^3, the mice were randomly divided into four groups (n = 6): PBS (60 μL), PBS + NIR (60 μL), GBN (2 mg/mL, 60 μL), GBN + NIR (2 mg/mL, 60 μL). After injection, tu-

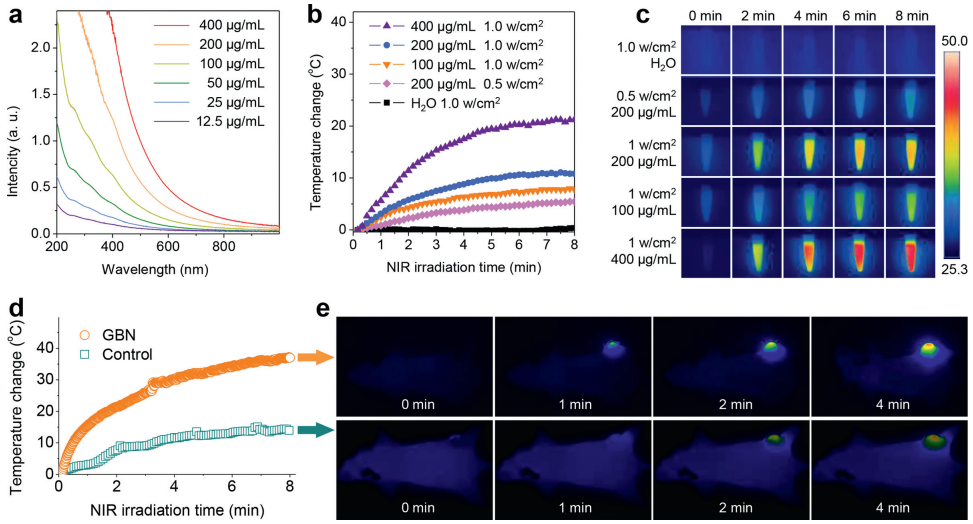

Fig. 2. Photothermal conversion performance of GBN. (a) UV-vis-NIR absorption spectra of GBN at varied concentrations (12.5, 25, 50, 100, 200, 400 μg/mL). Photothermal curves (b) and corresponding thermal imagings (c) of deionized water and aqueous solutions of GBN at different concentrations under irradiation with 808 nm laser at varied power densities. (d) Temperature change at the tumor sites of 4T1 tumor-bearing mice during laser irradiation, and corresponding infrared thermographic images (e).

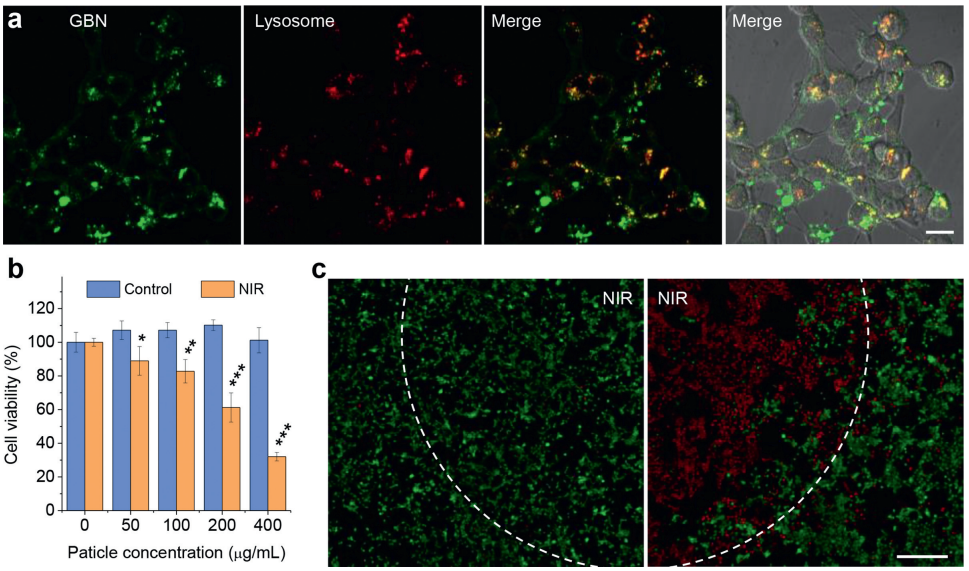

Fig. 3. The *in vitro* cytotoxicity and cellular uptake of GBN. (a) CLSM images of 4T1 cells after co-incubation with GBN for 4 h. (b) Viability of 4T1 cells with or without NIR irradiation. (c) The corresponding CSLM images (scale bar: 100 μm for all the panels) of 4T1 cells stained with calcein AM (live cells, green fluorescence) and PI (dead cells, red fluorescence) after different treatments. *P* values were calculated by one-way ANOVA with Tukey's post-test ($^{*}P < 0.05$, $^{**}P < 0.01$, $^{***}P < 0.001$) (For interpretation of the references to color in this figure legend, the reader is referred to the web version of this article.).

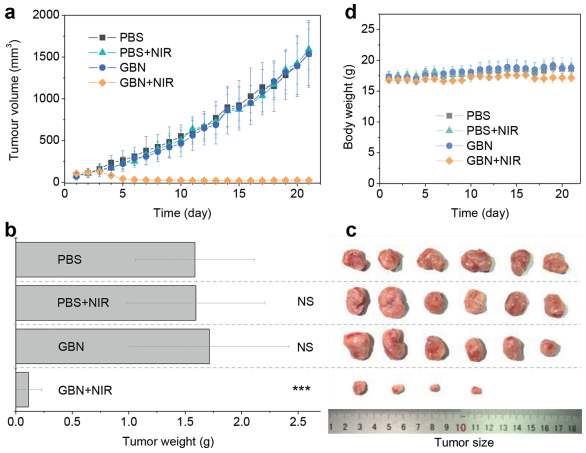

Fig. 4. GBN-mediated photothermal therapy of cancer *in vivo*. (a) Tumor growth curves of 4T1 tumor-bearing mice ($n = 6$, mean ± s.d.). (b) Body weight change of 4T1 tumor-bearing mice during treatment. (c) Tumor weight of mice after 21 days of treatment. (d) Corresponding digital photos of tumors harvested from mice after 21 days of treatment. Mean value and error bar are defined as mean and s.d., respectively. *P* values were calculated by one-way ANOVA with Tukey's post-test ($^{***}P < 0.001$; NS, no significance).

mors were immediately irradiated with 808 nm laser at the power density of 0.5 W/cm^2 for 5 min. Then, 5 min NIR irradiation was carried out two times again 1 day and 3 days after injection. After treatment for 21 days, all the treated mice survived, possibly owing to high bio-safety of GBN. From the collected everyday record by a digital caliper (Fig. 4a), neither GBN nor GBN−NIR groups induced tumor suppression compared to the blank control group of PBS, in which the tumor volumes reached up to 1500 mm^3 after 21 days treatment. By comparison, the GBN+NIR group showed effective inhibition to tumor growth (Figs. 4b and c), and even completely eradicated the tumors of some mice (Fig. 4c). In addition, Fig. 4d showed that there was no significant difference in body weight of 4T1 tumor-bearing mice between the four groups during treatment.

To further evaluate *in vivo* translation potential of GBN, a detailed investigation about *in vivo* toxicology of GBN was conducted. Twelve 4T1 tumor-bearing mice were randomly divided into four groups ($n = 3$) for treatment with PBS, PBS + NIR, GBN, GBN + NIR (2 mg/mL, 60 μL) and then collected the blood from mice orbit after two weeks. Blood biochemical analyses of the general hematologic parameters and liver functions and kidney functions were investigated. There was no statistically significant difference observed from both the hematologic parameters and blood biochemical indexes of GBN in comparison to the blank control group (Figs. S7 and S8 in Supporting information). These results demonstrated that the treatment with GBN did not generate negative impacts on physiological toxicity and blood chemistry. Besides, major organs, including heart, liver, spleen, lung and kidney, were collected after treatment and sliced for H&E staining for histological assay. It showed no obvious pathological change and adverse effects after 21 day treatment for all the groups, indicating no significant histological abnormality in the treatment group (Fig. S9 in Supporting information). These results suggested that GBN had a good biosafety in support of their future biomedical applications.

In conclusion, we have successfully synthesized a new type of gadolinium boride nanomaterials by the microwave-assisted chemical etching method. Importantly, we have uncovered fluorescence and NIR-photothermal properties of GBN, and demonstrated the cellular fluorescence imaging of GBN for cell trace and effective photothermal therapy of cancer. These important optical properties and good biocompatibility suggest that GBN might be a promising nanomaterial for biomedical applications.

Declaration of competing interest

The authors declare that they have no known competing financial interests or personal relationships that could have appeared to influence the work reported in this paper.

Acknowledgments

We greatly appreciate the help of the Instrumental Analysis Center of Shenzhen University (XiLi campus) for assistance in material characterizations. This work was sup-

ported by the National Natural Science Foundation of China (No. 51872188), Shenzhen Basic Research Program (Nos. JCYJ20170302151858466, JCYJ20170818093808351), Special Funds for the Development of Strategic Emerging Industries in Shenzhen (No. 20180309154519685), SZU Top Ranking Project (No. 860-00000210), and Hubei Key Laboratory of Plasma Chemistry and Advanced Materials for the Open Fund (No. 2020KF02).

Supplementary materials

Supplementary material associated with this article can be found, in the online version, at doi:10.1016/j.cclet.2021.04.036.

References

[1] Y.Y. Cheng, X.Y. Jiao, W.P. Fan, et al., Biomaterials 256 (2020) 120191.
[2] W. Sang, Z. Zhang, Y.L. Dai, X.Y. Chen, Chem. Soc. Rev. 48 (2019) 3771–3810.
[3] T.H. Kim, S. Lee, X.Y. Chen, Expert Rev. Mol. Diagn. 13 (2013) 257–269.
[4] L. Cheng, X.W. Wang, F. Gong, T. Liu, Z. Liu, Adv. Mater. 32 (2020) 1902333.
[5] R.X. Han, J.R. Peng, Y. Xiao, et al., Chin. Chem. Lett. 31 (2020) 1717–1728.
[6] Y.S. Chen, L. Li, W.J. Chen, H.Y. Chen, J. Yin, Chin. Chem. Lett. 30 (2019) 1353–1360.
[7] L. Li, Y.S. Chen, W.J. Chen, et al., Chin. Chem. Lett. 30 (2019) 1689–1703.
[8] X. Dong, H. Zhao, Y. Mi, et al., Chin. Chem. Lett. 31 (2020) 1616–1619.
[9] A. Zhang, L. Hai, T. Wang, et al., Chin. Chem. Lett. 31 (2020) 3158–3162.
[10] Q. Wang, Y.N. Dai, J.Z. Xu, et al., Adv. Funct. Mater. 29 (2019) 1901480.
[11] P.H. Zhao, Z.K. Jin, Q. Chen, et al., Nat. Commun. 9 (2018) 4241.
[12] A.R. Rastinehad, H. Anastos, E. Wajswol, et al., Proc. Natl. Acad. Sci. U. S. A. 116 (2019) 18590–18596.
[13] X.J. Huang, W.L. Zhang, G.Q. Guan, et al., Acc. Chem. Res. 50 (2017) 2529–2538.
[14] Z.K. Jin, D.Y. Chen, P.H. Zhao, et al., Theranostics 10 (2020) 1861–1872.
[15] Y.M. Wang, W. Feng, Y. Chen, Chin. Chem. Lett. 31 (2020) 937–946.
[16] M.J. Fan, Y.Y. Wen, D. Ye, et al., Adv. Healthc. Mater. 8 (2019) 1900157.
[17] B.Z. Xu, S.P. Beckman, 2D Mater 3 (2016) 031003.
[18] Y.F. Zhao, C.M. Ban, Q. Xu, S.H. Wei, A.C. Dillon, Phys. Rev. B Condensed Matter. 83 (2011) 035406.
[19] J. Nagamatsu, N. Nakagawa, T. Muranaka, Y. Zenitani, J. Akimitsu, Nature 410 (2001) 63–64.
[20] A. Pediaditakis, M. Schroeder, V. Sagawe, T. Ludwig, H. Hillebrecht, Inorg. Chem. 49 (2010) 10882–10893.
[21] H. Nishino, T. Fujita, N.T. Cuong, et al., J. Am. Chem. Soc. 139 (2017) 13761–13769.
[22] X.J. Men, F. Wang, H.B. Chen, et al., Adv. Funct. Mater. 30 (2020) 1909673.
[23] R. Zhu, L.C. Su, J.Y. Dai, et al., ACS Nano 14 (2020) 3991–4006.
[24] D.K. Roper, W. Ahn, M. Hoepfner, J. Phys. Chem. C 111 (2007) 3636–3641.
[25] L. Zhang, D. Sheng, D. Wang, et al., Theranostics 8 (2018) 1591–1606.